DYNAMIC FLUID SHEAR SRRESS MEASUREMENTS ON THE NORMAL AORTIC VALVE LEAFLET USING LASER DOPPLER VELOCIMETRY

A Thesis
Presented to
The Academic Faculty

by

Gowthami Tamilselvan

In Partial Fulfillment
Of the Requirements for the Degree
Bachelor of Science with Research Option in the
School of Chemical and Biomolecular Engineering

Georgia Institute of Technology
April 2011

Dynamic Fluid Shear Stress Measurements on the Normal Aortic Valve Leaflet Using Laser Doppler Velocimetry

Gowthami Tamilselvan
Undergraduate Student
School of Chemical and Biomolecular Engineering
Georgia Institute of Technology, Atlanta, Georgia

Choon Hwai Yap
Research Mentor
Wallace H. Coulter School of Biomedical Engineering,
Georgia Institute of Technology, Atlanta, Georgia

Dynamic Fluid Shear Stress Measurements on the Normal Aortic Valve Leaflet Using Laser Doppler Velocimetry

Approved by:

_____

Dr. Ajit Yoganathan
The Wallace H. Coulter Distinguished Faculty Chair in Biomedical Engineering and Regents Professor Associate Chair for Research
School of Chemical and Biomolecular Engineering
Georgia Institute of Technology and Emory University

Dynamic Fluid Shear Stress Measurements on the Normal Aortic Valve Leaflet Using Laser Doppler Velocimetry

Approved by:

_____

Dr. Clifford Henderson
Associate Professor
GT ChBE Undergraduate Research Coordinator
School of Chemical and Biomolecular Engineering
Georgia Institute of Technology

Dynamic Fluid Shear Stress Measurements on the Normal Aortic Valve Leaflet Using Laser Doppler Velocimetry

Approved by:

_____

Dr. Pradeep Agrawal
Professor and Associate Chair for Undergraduate Program
School of Chemical and Biomolecular Engineering
Georgia Institute of Technology

ACKNOWLEDEMENTS

I would like to thank my research advisor, Dr. Ajit Yoganathan, for providing me the opportunity to work in the Cardiovascular Fluid Mechanics Laboratory. He has been a great advisor and working in this lab has provided valuable experiences to take with me. I like to express my heartfelt gratitude to my research mentor, Choon Hwai Yap, for his inspiration, encouragement and great efforts to teach me everything I needed to know. He helped me become more independent and a responsible researcher. This paper would not have been possible without his guidance and advice. I am grateful to all the members of the Cardiovascular Fluid Mechanics Laboratory for all their help and support.

TABLE OF CONTENTS

ACKNOWLEDEMENTS **6**

LIST OF TABLES AND FIGURES **8**

ABSTRACT **9**

INTRODUCTION **10**

METHODOLOGY **12**

Valve Model 12

Chamber Model 13

Laser Doppler Velocimetry 14

Shear Stress 15

RESULTS AND DISCUSSION **16**

Pressure 16

Flow 16

Leaflet location 17

Shear stress 19

DISCUSSION **23**

CONCLUSION **25**

REFERENCES **26**

LIST OF TABLES AND FIGURES

Figure 1: Normal aortic valve and a calcified aortic valve. 10

Figure 2: Mechanical Forces. 11

Figure 3: Native porcine valve sutured onto a plastic ring with three stents 12

Figure 4: Acrylic chamber with three-lobed idealized sinus geometry 13

Figure 5: Schematic diagram of the pulsatile flow loop 14

Figure 6: Graph of the pressure across the valve in the flow loop 16

Figure 7: Flow waveform for various stroke volumes 17

Figure 8: Flow waveform for various heart rates 17

Figure 9: Reflected light intensity map of the leaflet 18

Figure 10: Leaflet position for various stroke volumes 19

Figure 11: Leaflet position for various heart rates 19

Figure 12: Shear stress over the cardiac cycle 20

Figure 13: Shear stress at various stroke volumes 21

Figure 14: Shear stress at various heart rates 22

Figure 15: Flow in the sinus area 23

Table 1: Peak shear stress for the four different stroke volumes 21

Table 2: Peak shear stress for the three different heart rates 22

ABSTRACT

Aortic valve (AV) calcification is a major cause of mortality and morbidity. This disease involves the chronic inflammation of the AV leaflets and calcium deposition, resulting in valve stenosis and regurgitation. The exact cause of aortic valve calcification is unknown but previous studies have shown that adverse mechanical forces play a role.[1] Unfortunately, the mechanical environment of the AV is not well known. Thus, the objective of this project was to make experimental measurements of the fluid shear stress mechanical environmental of the native aortic valve. Native aortic valves were excised from porcine hearts, sutured onto stented rings, and tested in an *in vitro* pulsatile flow loop. Laser Doppler Velocimetry (LDV) was used to measure shear stresses on the aortic surface of the valve leaflet. Two fluid shear stress experiments were run to understand the effects of hemodynamics on fluid shear stress: varying stroke volumes at a constant heart rate and varying heart beats at a constant stroke volume. As the stroke volume increased, fluid shear stresses increased due to the stronger sinus fluid motion. As the heart rate increased, fluid shear stresses decreased due to reduced systolic duration which restricted strong sinus flow formations. These results show that a higher heart rate can potentially elicit sclerotic responses from the AV and a higher velocity may reduce sclerotic responses from the AV. This data can be used to further understand AV biological response to shear stresses and to create improved computational simulations of flow dynamics in an aortic valve.

KEY WORDS: Native aortic valve, aortic valve leaflet, fluid shear stress, Laser Doppler Velocimetry

INTRODUCTION

The aortic valve (AV) regulates blood flow from the left ventricle to the aorta, which leads to the rest of the body. Calcific aortic valve disease is one of the most common heart valve diseases, affecting 2% of the elderly population.[2] AV leaflets experience chronic inflammation, which results in calcification (deposits of calcium) on the cusps as shown in Figure 1. Calcification may result in aortic stenosis, regurgitation and eventually heart failure, or other catastrophic problems such as aneurysms and dissections.[3] Aortic stenosis is the narrowing of the aortic valve opening, which causes the heart to pump harder to overcome resistance so thus increasing pressure.[4] Regurgitation is the backflow of blood due to incompetent valve closure.

Figure 1: Normal aortic valve (left image) and a calcified aortic valve (right image).[19]

It has been hypothesized that exposure to adverse mechanical forces may be the cause of early calcification to the valve leaflets. Specifically, fluid shear stress protects against pro-inflammatory and pro-oxidative expressions in valvular endothelial cells.[5] In addition, reduced shear stresses on the non-coronary leaflet of the AV increases the risk of aortic valve calcification.[20] *Ex vivo* studies indicated that mechanical forces influence valve biology and pathobiology and thus could play a role in the development of calcific aortic valve disease. Figure 2 displays the mechanical forces on the valve. Previous studies have suggested that the leaflets are sensitive to their mechanical environment depending on the magnitude of fluid shear

stress.[6,7] In order to verify this hypothesis, the mechanical environment of the normal aortic valve must be fully characterized.

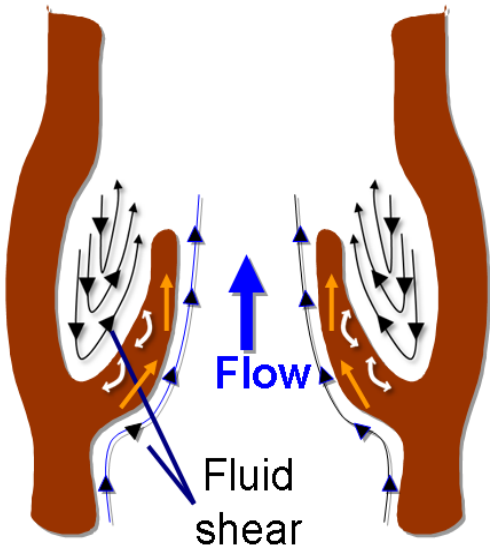

Figure 2: Mechanical forces on the valve.[8]

The objective of the current study was to obtain experimental measurements of the mechanical environment of the normal aortic valve, more specifically, fluid shear stresses on the leaflets of the valve using Laser Doppler Velocimetry (LDV). This study examined the effects of hemodynamics (various stroke volumes and heart rates) on AV fluid shear stresses. The shear stress data gathered from the experiment will help identify the effects of fluid shear on valve biology and calcification. Additionally, these results can be used to numerically model flow dynamics in the aortic valve. Subsequently, modeling of the motion of the valve can become more accurate to match native physiology. Finally, understanding the valve environment will facilitate the development of improved tissue engineered aortic valves.

METHODOLOGY

Shear stress measurements were conducted over a range of varying stroke volumes and heart rates to understand the effects of hemodynamics on shear stresses. Four different stroke volumes were studied: 29 ml, 43 ml, 62 ml, and 68 ml. Three different heart rates were also studied: 50, 70 and 90 beats/minute. These values were chosen to cover a range of physiological conditions as heart rate and stroke volume differs between race, gender and age.

Valve Model

Native aortic valves were constructed from porcine tissues, and tested in a pulsatile flow loop. Porcine hearts were obtained from the local slaughterhouse (Holifield Farms, Covington, GA) and the aortic root was removed and trimmed. The sinus wall of the root was excised and sutured to a dual-stented plastic ring as shown in Figure 3. The valve is placed in a 0.1% gluteraldehyde solution for 24 hours under mild aortic pressure of 25 mmHg. This procedure ensured that the valve did not degrade while undergoing experiments.

Figure 3: Native porcine valve sutured onto a plastic ring with three stents.

Chamber Model

A normal chamber was made using idealized sinus geometries from previous experimentation. Figure 4 shows the chamber design. The valve was positioned into this acrylic chamber ensuring that there is no gap between the stents and the walls of the chamber.

Figure 4: Acrylic chamber with three-lobed idealized sinus geometry.

The AV model was tested using the Georgia Tech Left Simulator as the pulsatile flow loop as shown in Figure 5. The flow loop was capable of replicating the physiological hemodynamic conditions of the human heart. This includes cardiac output at 5 liters per minute, 35% systolic duration to cardiac cycle ratio, and aortic pressure of 120/80 mmHg. The loop contains the aortic chamber with the valve, reservoir, pump and a pulse programmer which controls the heart rate. The solution in the flow loop is 36% glycerine and 64% water, and has a kinematic viscosity approximately of 3.5 mm^2/s (equivalent to the viscosity of blood).

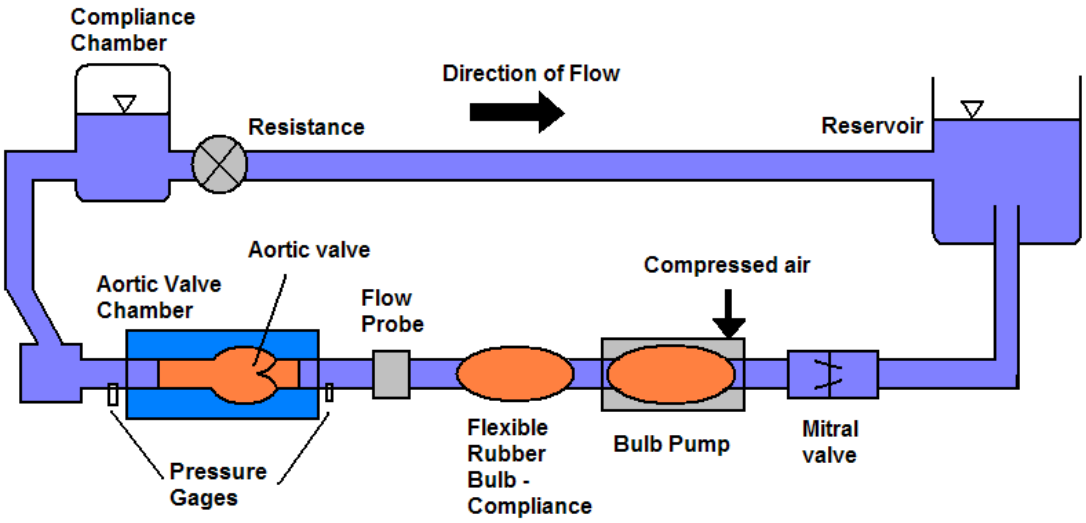

Figure 5: Schematic diagram of the Georgia Tech Left Simulator.

Laser Doppler Velocimetry

Two-dimensional velocity was measured in the valve model using a three-component, fiber optic, coincident Laser Doppler Velocimetry (LDV) system (Aerometric System, TSI Inc., Shoreview, MN). A 4W Argon-ion single laser beam, attached to a fiber drive unit, was split into two beams, which were focused at the measurement location. Intersection of the two beams caused interference and produced a set of straight fringes. As particles flowed through this segment, they reflected light with a signature scatter pattern known as the Doppler burst. This was processed by the Fast Fourier Transform based real-time analyzers (RSA-1000, TSI Inc., Shoreview, MN). The fiber drive unit was connected to a two-component fiber optic transceiver probe, which had a focal length lens of 100 mm. The optical density between the flow loop fluid and air is 19μm by 126 μm. All measurements were acquired in the backscatter mode in which a single probe transmitted and received the Doppler signals. The LDV system was set to a sampling frequency of 5 MHz and thus a velocity resolution of 1.8 cm/s. The pulse programmer received all data to phase lock the measurements to the cardiac cycle. From the characteristics of

the Doppler burst, velocities at the measured location were calculated. 40,000 data points were taken at each position.

Measurements were taken from the sinus wall to the surface of the valve leaflet along the radial line. Measurements were also taken downstream from the valve. To account for flow loop fluid optical density, consecutive measurement points were 89 μm apart. At each point, velocity measurements were binned into 86 phases of 10 ms each over the entire cardiac cycle. Shear stress was calculated by computing the velocity profile gradient at the leaflet surface. The laser was adjusted to provide the greatest intensity for every experiment. A data acquisition system was used to measure the intensity of the laser for each measurement; 40 cycles were recorded for each point. MATLAB was used to analyze data and calculate shear stress.

Shear Stress

Two assumptions were made in computing shear stress: Newtonian mechanics is valid and the fluid is Newtonian and isotropic. Shear stress was calculated using Equation 1.

$$\tau_{ij} = \mu\left(\frac{\delta u_i}{\delta x_j} + \frac{\delta u_j}{\delta x_i}\right) \quad (1)$$

τ is the shear stress, μ is the fluid's dynamic viscosity, u_i is the ith component of the velocity and x_i is the position of ith axis. The stream-wise direction was represented as i and the radial direction as j. The first term in the equation can be found from the taking the gradient of the stream-wise velocity with respect to the radial distance, which was measured using LDV. The second term was neglected; this value represented the dynamics of the valve leaflet but its magnitude was negligible in most cases.

RESULTS

Pressure

The aortic pressure was maintained at 120/80 mmHg in the flow loop. Figure 6 shows a representative pressure waveform at a heart rate of 70 beats/min and stroke volume of 62 ml. This pressure curve was similar for the other conditions (various stroke volumes and heart rates).

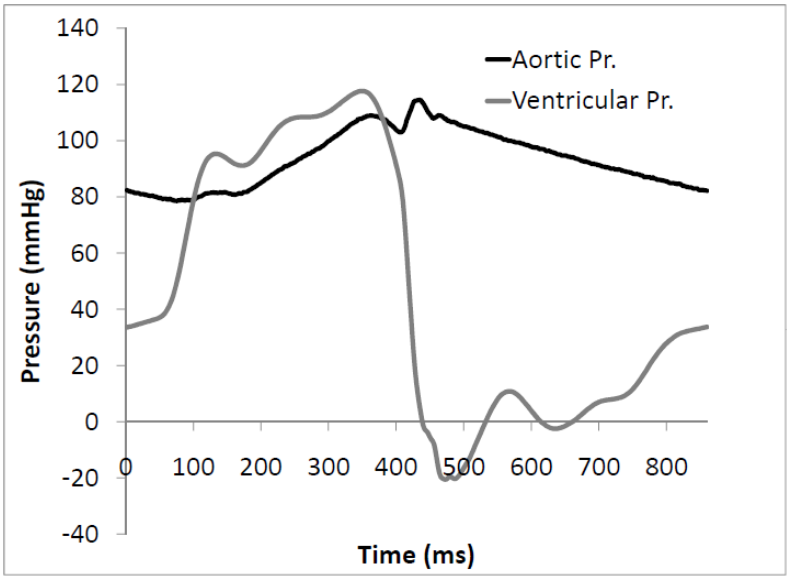

Figure 6: Graph of the pressure across the valve in the flow loop.

Flow

Systolic flow waveforms were found for the different conditions stated previously. Figure 7 displays the graph for different stroke volumes at a heart rate of 70 beats/min. As stroke volume increased, volumetric flow rate also increased. Figure 8 shows the graph for different heart rates at a stroke volume of 55 ml. As heart rate increased, systolic duration decreased. For the heart rate of 90 beats/min, bulk forward flow was higher than the other heart rates during early systole and lower in late systole.

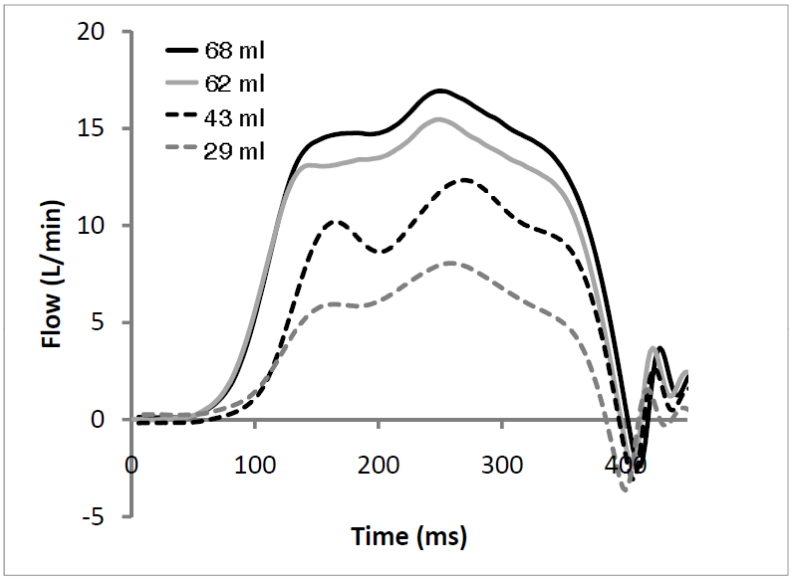

Figure 7: Flow waveform for various stroke volumes.

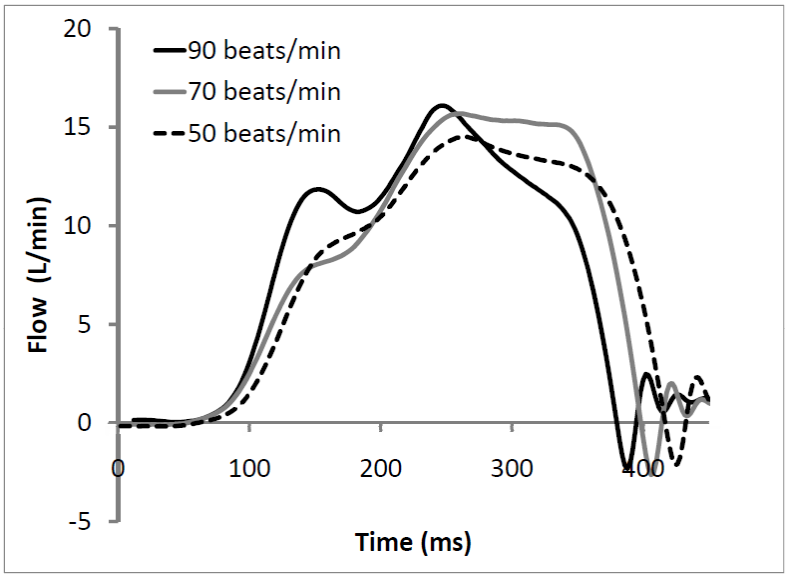

Figure 8: Flow waveform for various heart rates.

Leaflet location

To compute shear rate, the leaflet location and orientation was first calculated. Using the data acquisition system, the back-scattered laser light was recorded from the LDV probe. The intensity of reflected light was highest when the leaflet was within the probe volume. Figure 9 represents the back-scattered light intensity map over time, which displays the trajectory of the valve leaflet during systole. At 100 ms, the leaflet is opened and at 400 ms, it is closed.

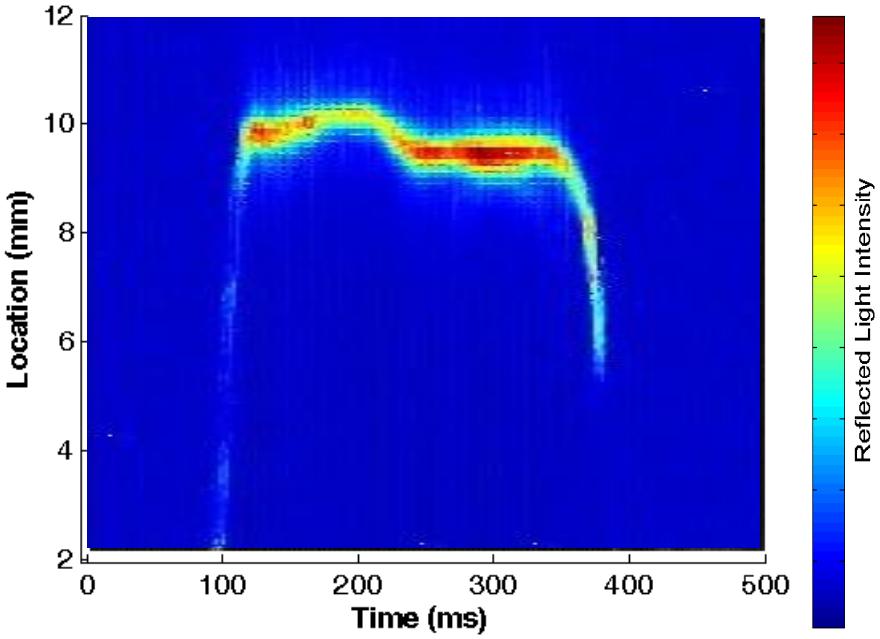

Figure 9: Reflected light intensity map of the leaflet.

Using the reflected light intensity technique, systolic positions of the leaflet were graphed for the different conditions. Figure 10 shows the leaflet location for various stoke volumes and Figure 11 for the various heart rates. All conditions followed a similar trend; leaflet is opened further during early systole than late systole. In Figure 10, the systolic leaflet positions for the various stroke volumes were less than 1 mm away from each other. For the leaflet position of the 29 ml stroke volume, the valve leaflets closed earlier due to shorter systolic duration as compared to the others. In Figure 11, 50 beats/min and 70 beats/min were similar in shape. However, for 90 beats/min the valve leaflets opened slightly further away from the sinus and it closed earlier. This was due to a decrease in systolic duration at a higher heart rate than the other two cases.

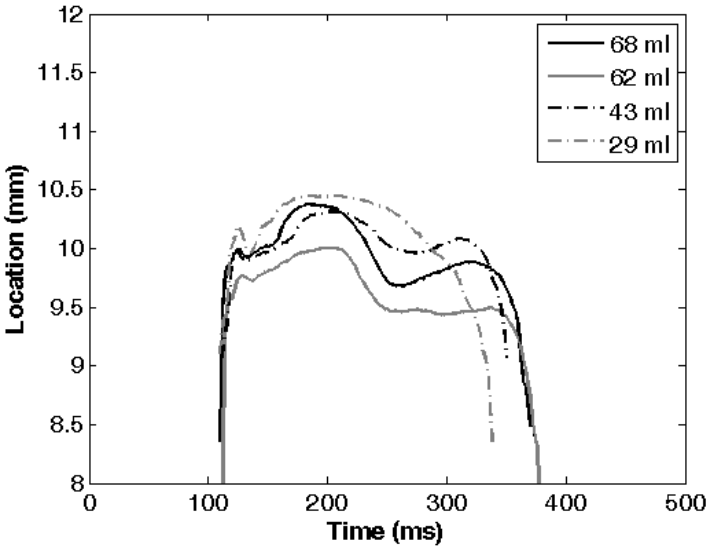

Figure 10: Leaflet position for various stroke volumes.

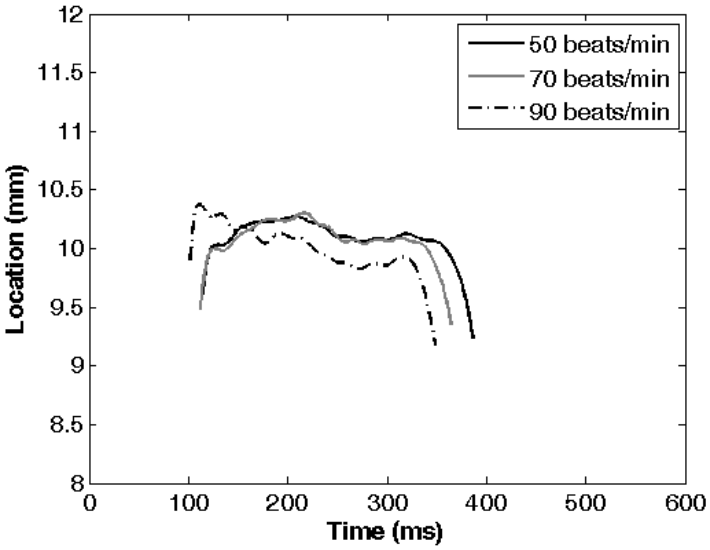

Figure 11: Leaflet position for various heart rates.

Shear stress

Shear stress experienced by the aortic valve was calculated for the entire cardiac cycle. Figure 12 displays the shear stress experienced by the leaflet under a heart rate of 70 beats/min and stroke volume of 73 ml. Shear stress was higher during systole than diastole as shown in the graph. Shear stress was low in the beginning, quickly raised to about 21 dyn/cm^2 at mid systole and rapidly decreased after its peak. Shear stress started at approximately 3 dyn/cm^2 for diastole

and decreased to zero. Since the systolic region is more prominent than the diastolic region, this study only focused on the systolic shear stresses.

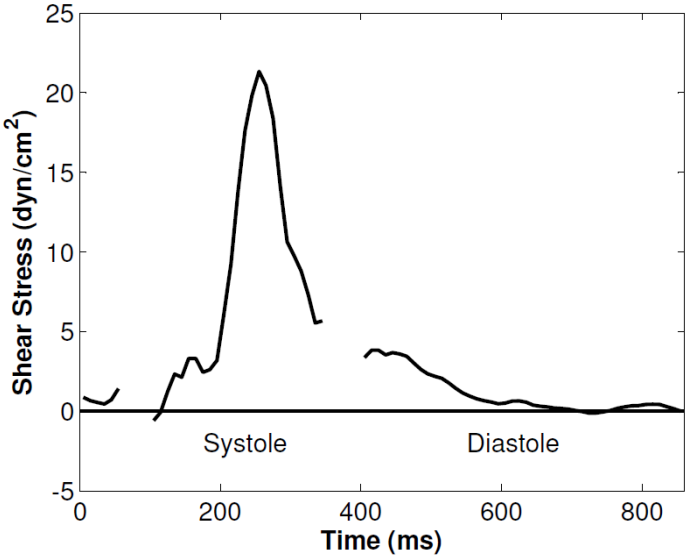

Figure 12: Shear stress over the cardiac cycle.

Shear stress waveforms over systole were graphed for the different conditions. Figure 13 shows the shear stress of different stroke volume for the same heart rate of 70 beats/min. Table 1 displays peak shear stress for the four different conditions. For the four stroke volumes, shear stress was low during early systole and increased during late-mid to early-end systole. In early systole, immediately after valve opening, a small negative peak was observed in all of the conditions. This negative value approached zero as stroke volume increased. Peak shear stress was seen around 275 ms and declined to zero at approximately 350 ms. Shear stress ranged from 1.1 dyn/cm^2 for stroke volume of 29 ml to 15 dyn/cm^2 for stroke volume of 68 ml. As the stroke volume increased, systolic shear stress also increased. A larger stroke volume resulted in more bulk forward flow rate, which induced stronger sinus vortices.

Table 1: Peak shear stress for the four different stroke volumes.

Heart Rate (beats/min)	Stroke Volume (ml)	Peak Shear Stress (dyn/cm^2)
70	68	15.0
70	62	13.4
70	43	6.4
70	29	1.1

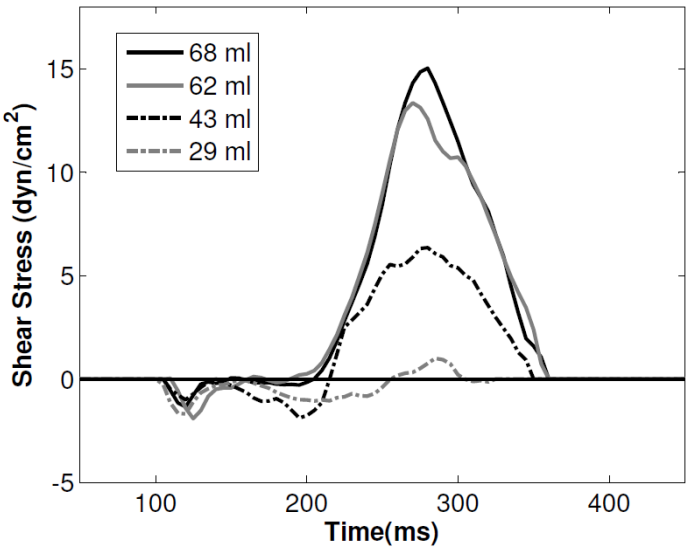

Figure 13: Shear stress at various stroke volumes.

Figure 14 shows the shear stress of different heart rates for the same stroke volume of 55 ml. Table 2 displays the peak shear stress for the various heart rates. During early systole, a negative peak was seen; this peak increased as the heart rate increased. Heart rates of 50 beats/min and 70 beats/min were similar in shape, and unlike the 90 beats/min. 70 beats/min had a lower late systolic peak shear stress than the 50 beats/min. At the higher heart rate, the initial low shear stress was not seen; however, a rather quick increase in shear stress to an early systolic peak of approximately 5 dyn/cm^2 occurred. After this, shear stress decreased slightly and rose back up to about 7 dyn/cm^2. As heart rate increased, systolic shear stress decreased and bulk forward flow increased. Higher heart rate resulted in shorter systolic duration; this reduced the time for high velocities to form in the sinus, resulting in a lower shear stress. Figure 8 and 11 show that when the heart rate is at 90 beats/min, the leaflet opened wider and a larger bulk

forward flow rate existed during early systole. This behavior lead to early systolic elevation of positive shear stress for this case. Shear stress was reduced during late systole because the leaflet opened narrower and a lower bulk forward flow rate existed.

Table 2: Peak shear stress for the three different heart rates.

Heart Rate (beats/min)	Stroke Volume (ml)	Peak Shear Stress (dyn/cm^2)
50	55	11.4
70	55	10.2
90	55	7.8

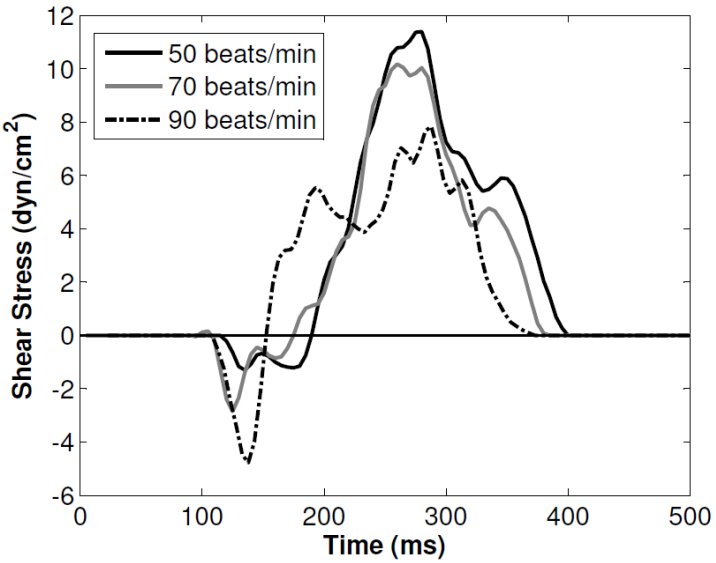

Figure 14: Shear stress at various heart rates.

DISCUSSION

Behavior of shear stress can be understood by the interaction between sinus flow and valve leaflets. The flow and fluid in the sinus volume determines the formation of sinus vortices depending on the valve opening angle. In Figure 15, the valve opening is less than 90^{O}, so a strong sinus vortex is formed due to the entrainment of the calm sinus flow. The forward flow jet induces sinus flow by drag forces causing a shear stress peak after a large delay. In Figure 12, shear stress decreased after reaching its peak because of viscous energy dissipation and deceleration of forward flow; this reduces the intensity of the sinus vortex.

In Figure 12 during diastole, shear stress decreased to zero. This occurs during late systole, where there is a reverse in flow due to pressure gradient, which subsequently results in fluid mixing. This causes remnant fluid motion distal to the valve, which disperses over the diastolic duration through viscous interactions.

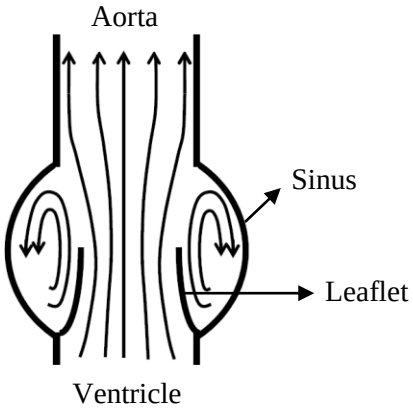

Figure 15: Flow in the sinus area.

Only one previous study has measured the fluid shear stress on a polymeric valve leaflets. However, it studied steady flow conditions and temporal resolution was not measured.[9] In addition, magnetic resonance imaging and cardiac ultrasound were used to measure the mechanical environment of the aortic valve. However, these methods do not provide the spatial

and temporal resolution that can be achieved using these *in vitro* stress measurement techniques. In addition to improving computational simulations, this shear stress data can be used in mechanobiology experiments to study the development of calcification.

By studying the various conditions, it was found that aortic surface shear stress is strongly influenced by hemodynamic parameters. This means that if any disease or condition influences changes in hemodynamics, then aortic surface shear stresses will be affected. Currently, the exact method of how changes in shear stresses affect aortic valve biology is unknown. However, further *in vitro* studies can be conducted to understand this mechanism. Previous studies have shown that low and oscillatory shear stresses lead to vascular endothelium sclerosis.[10-12] If shear stress on aortic valve endothelium is similar to vascular endothelium, then a higher heart rate may minimize shear stress potentially eliciting sclerotic responses from the aortic valve. Tachycardia is a disorder when the heart beats faster than normal, which increases the risk for heart disease.[13-14] Studies have shown that tachycardia and hypertension are closely linked and hypertension increases the risk of aortic valve calcification.[15-18]

CONCLUSION

Shear stress measurements were taken on the aortic surface of the aortic valve leaflet. Shear stress is higher for the systolic region than the diastolic region. As stroke volume increased, systolic shear stresses also increased. As heart rate increased, systolic shear stresses decreased. Systolic shear stress increased with wider valve leaflet opening.

Using the methodology described, these *in vitro* experiments can be run under different parameters to manipulate various heart conditions. Instead of a normal aortic valve, a bicuspid valve (BAV) model can be studied in the pulsatile flow loop. Shear stress measurements can be calculated for any condition that needs further investigation.

REFERENCES

1. Butcher, J.T., et al. (2006), Transcriptional profiles of valvular and vascular endothelial cells reveal phenotypic differences: influence of shear stress. A*rterioscler Thromb Vasc Biol,* 26, 69-77.
2. Lindroos, M., M. Kupari, J. Heikkila and R. Tilvis (1993), Prevalence of aortic valve abnormalities in the elderly: an echocardiographic study of a random population sample. *J Am Coll Cardiol,* 21(5), 1220-1225.
3. "Bicuspid Aortic Disease." *Cedars-Sinai*. Thoracic Aortic Surgery Program, n.d. Web. 14 Sep 2010. <http://www.cedars-sinai.edu/Patients/Programs-and-Services/Heart-Institute/Treatment-Programs/Bicuspid-Aortic-Disease.aspx>.
4. Hahn, Rebecca. "Association of Aortic Dilation with Regurgitant, Stenotic and Functionally Normal Bicuspid Aortic Valves." American College of Cardiology. (1992).
5. Butcher, J.T., et al. (2006), Transcriptional profiles of valvular and vascular endothelial cells reveal phenotypic differences: influence of shear stress. A*rterioscler Thromb Vasc Biol,* 26, 69-77.
6. Sucosky, P., et al. (2009), Altered shear stress stimulates upregulation of endothelial VCAM-1 and ICAM-1 in a BMP-4- and TGF-beta1-dependent pathway. *Arterioscler Thromb Vasc Biol*, 29, 254-260.
7. Xing, Y., et al. (2004), Cyclic pressure affects the biological properties of porcine aortic valve leaflets in a magnitude and frequency dependent manner. *Ann Biomed Eng*, 32, 1461-1470.
8. Tissue engineered heart valve (tehv) project. (n.d.). Retrieved from http://www.bme.gatech.edu/groups/cfmg/group/TEHV%20Project.html

9. Weston, M. W., D. V. LaBorde and A. P. Yoganathan (1999). Estimation of the shear stress on the surface of an aortic valve leaflet. *Ann Biomed Eng*, 27(4), 572-579.
10. Rossi, P., Granel, B., Marziale, D., Le Mée, F. and Francès, Y. (2010), Endothelial function and hemodynamics in systemic sclerosis. Clinical Physiology and Functional Imaging, 30: 453–459. doi: 10.1111/j.1475-097X.2010.00965.x
11. Ku, D. N., D. P. Giddens, C. K. Zarins and S. Glagov (1985). Pulsatile flow and atherosclerosis in the human carotid bifurcation. Positive correlation between plaque location and low oscillating shear stress. *Arteriosclerosis*, 5(3), 293-302.
12. Chatzizisis, Y. S., A. U. Coskun, M. Jonas, E. R. Edelman, C. L. Feldman and P. H. Stone (2007). Role of endothelial shear stress in the natural history of coronary atherosclerosis and vascular remodeling: molecular, cellular, and vascular behavior. *J Am Coll Cardiol*, 49(25), 2379-2393.
13. Kannel, W. B., C. Kannel, R. S. Paffenbarger, Jr. and L. A. Cupples (1987). Heart rate and cardiovascular mortality: the Framingham Study. *Am Heart J*, 113(6), 1489-1494.
14. Palatini, P. (1999). Elevated heart rate as a predictor of increased cardiovascular morbidity. *J Hypertens Suppl*, 17(3), S3-10.
15. Levy, R. L., P. D. White and et al. (1946). Transient tachycardia; prognostic significance alone and in association with transient hypertension. *Med Press Egypt*, 38(6), 207-212.
16. Palatini, P., E. Casiglia, P. Pauletto, J. Staessen, N. Kaciroti and S. Julius (1997). Relationship of tachycardia with high blood pressure and metabolic abnormalities: a study with mixture analysis in three populations. *Hypertension*, 30(5), 1267-1273.
17. Pate, G. E. (2002). Association between aortic stenosis and hypertension. *J Heart Valve Dis*, 11(5), 612-614.

18. Rabkin, S. W. (2005). The association of hypertension and aortic valve sclerosis. *Blood and Press*, 14(5), 264-272.

19. "Patients." *Valvexchange, Inc.* n. pag. Web. 18 Apr 2011. <http://www.valvexchange.com/patients/index.html>.

20. Freeman, R. V. and C. M. Otto (2005). Spectrum of calcific aortic valve disease: pathogenesis, disease progression, treatment strategies. *Circulation*, 111(24), 3316-3326.